Organic LETTERS

Letter

pubs.acs.org/OrgLett

Efficient Approach to Electron-Deficient 1,2,7,8-Tetraazaperylene Derivatives

Ruizhi Tang,[†] Fan Zhang,*[,†] Yubin Fu,[†] Qing Xu,[†] Xinyang Wang,[†] Xiaodong Zhuang,[†] Dongqing Wu,[†] Angelos Giannakopoulos,[‡] David Beljonne,[‡] and Xinliang Feng*[,†,§]

[†]School of Chemistry and Chemical Engineering, State Key Laboratory of Metal Matrix Composites, Shanghai Jiao Tong University, Shanghai 200240, P. R. China

[‡]Université de Mons - UMONS/Materia Nova, Place du Parc, 20, B-7000 Mons, Belgium

[§]Max-Planck Institute for Polymer Research, Ackermannweg 10, 55128, Mainz, Germany

Supporting Information

ABSTRACT: Using an efficient synthetic strategy, a novel class of 1,2-diazine-embedded perylenes, namely 1,2,7,8-tetraazaperylene derivatives, have been successfully synthesized. These molecules were fully characterized by X-ray diffraction analysis, optical spectroscopy, and electrochemistry. The low-lying lowest unoccupied molecular orbital (LUMO) level of these molecules suggests their potential as good electronic acceptors.

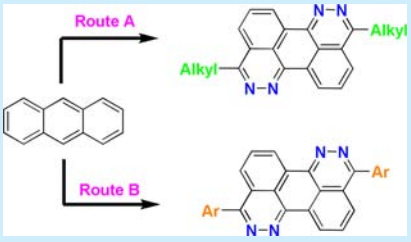

Because of their excellent optoelectronic properties, polycyclic aromatic hydrocarbons (PAHs) have gained increasing interest concerning their synthetic protocols and potential applications in optoelectronic devices, such as organic field transistors (OFETs), organic solar cells (OPVs), and organic light-emitting devices (OLEDs).[1] The conjugated backbone of PAHs consists of multifused aromatic rings and possesses different edge structures that determine their intrinsic chemical and physical properties.[2] Incorporation of heteroatoms into the aromatic frameworks of PAHs has proven to be an efficient strategy for tuning the molecular energy level and intermolecular interactions. Thanks to the matched atom radiometer and electronegativity, the nitrogen atom is an amazing element for building up various functional PAHs, e.g., N-heteroacences. As a consequence, an improved resistance to degradation (oxidation or dimerization) for heteroacences, as compared with their full-carbon based analogues, enables them to serve as stable n-type semiconducting materials.[3]

Perylene (**I**) is a typical rylene-type PAH, structurally featured with armchair and zigzag edges or peri and bay regions (Figure 1). It exhibits a rigid planar structure, good chemical stability, and rich optical properties.[4] The bay regions can be chemically modified by incorporating additional heteroatoms, leading to an extended π-conjugated backbone, e.g., 1,2,7,8-tetraazacoronene (**II**) via the Diels–Alder reaction,[5] and dithioperylene (**III**) by fusing two sulfur atoms.[6] Another example of rylene derivatives, i.e., 7,8,15,16-tetraazaterrylene (**IV**) can be readily prepared, and it exhibits electron-deficient character as well as one-dimensional columnar stacking in bulk.[7] Despite the remarkable achievements in the synthesis of various functional perylene derivatives, the preparation of aza-perylene by replacing carbon atoms with heteroatoms in the conjugated framework has been rarely reported.

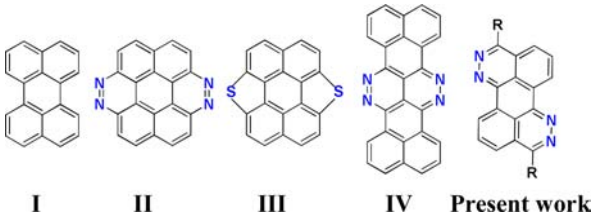

Figure 1. Typical examples of perylene derivatives.

Herein, we present an efficient approach toward unprecedented electron-deficient 1,2,7,8-tetraazaperylene derivatives by incorporating two diazine moieties into the perylene backbone. The geometric and electronic structures of the resulting molecules were fully characterized by optical spectroscopy, cyclic voltammetry, and X-ray single-crystal analysis.

Scheme 1 illustrates the synthetic strategy toward the target compounds. The attachment of alkyl chains to the tetraazaperylene backbone was performed by a concise protocol. As an example, the reaction of anthracene with hexanoyl chloride using $AlCl_3$ as catalyst yielded mixed isomers of 1, 5-dihexanoylanthracene **2a** and 1,8-dihexanoylanthracene in a ratio of nearly 1:1. Further purification by recrystallization and flash chromatography afforded pure **2a** in 36% yield.[8] Afterward, the intermediate compound **2a** was subjected to oxidation by CrO_3, giving the key intermediate **3a** in a nearly quantitative yield. Finally, upon treatment of **3a** with hydrazine hydrate, the target compound **4a** was achieved in 95% yield. Applying the similar synthetic

Received: July 17, 2014
Published: September 3, 2014

dx.doi.org/10.1021/ol502109y | Org. Lett. 2014, 16, 4726–4729

Scheme 1. Synthesis of 1,2,7,8-Tetraazaperylene Derivatives

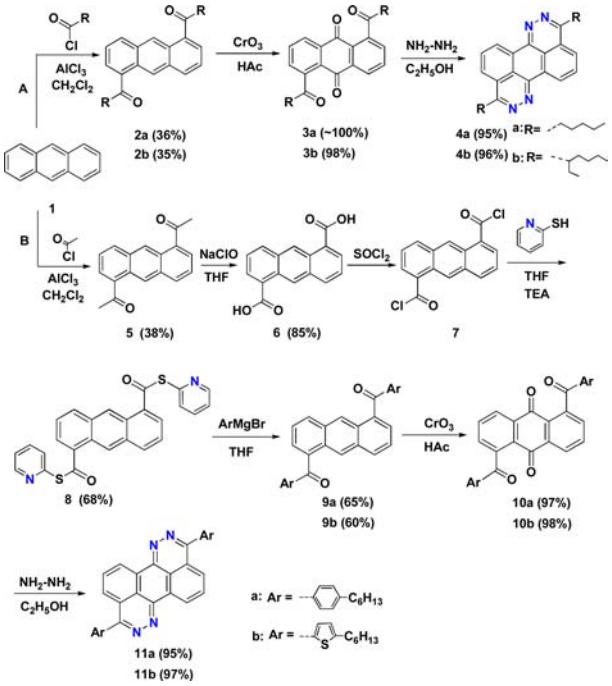

procedure, compound **4b** substituted with branched side alkyl chain was synthesized in an overall yield of 32.9%.

Next, we attempted to introduce aryl groups on 1,2,7,8-tetraazaperylene core with the aim to achieve the extended conjugation. Unfortunately, the treatment of aroyl chloride with anthracene did not yield the expected aryrylanthracene intermediates. Thus, it is difficult to synthesize aryl substituted tetraazaperylene based on the route described above. Hence, we turned to an alternative synthetic protocol based on the key compound **6** (1,5-anthracenedicarboxylic acid),[9] which was obtained from anthracence in two steps (Scheme 1B). Compound **6** was readily converted into **7** (1,5-anthracenedicarbonyl dichloride) after treatment with $SOCl_2$. Since compound **7** could not be directly converted into **9** by reacting with an aryl Grignard reagent, a good leaving group, the *S*-pyridinyl substituent, was introduced to replace the chloride group by the treatment of **7** with 2-mercaptopyridine, using triethylamine (TEA) as a catalyst, affording compound **8** as a pale-yellow solid in 68% yield. After further reaction with arylmagnesium bromide in THF at 0 °C and stirring overnight, compounds **9a** and **9b** with 4-hexylphenyl and 4-hexylthienyl substitutions were obtained in 65% and 60% yield, respectively. Upon oxidation with CrO_3, compounds **10a** and **10b** were obtained in nearly quantitative yields and then readily converted to target molecules **11a** and **11b** in very high yields (more than 95%), respectively, after treatment with hydrazine hydrate. All new compounds were fully characterized by ^1H and ^{13}C NMR spectroscopy and high-resolution mass spectroscopy, verifying the chemical identity of the compounds (Supporting Information). Specifically, in ^1H NMR spectra, one set of proton signals can be observed for all target molecules, indicating their highly symmetric structures. It is worth mentioning that some pivotal intermediates achieved here, such as 1,5-diacyl-substituted anthraquinone derivatives (**3a**,**b** and **10a**,**b**) might be suitable for constructing other expanded polyaromatic systems with complex structures.[10]

The structure of compound **4a** was further confirmed by X-ray crystallographic analysis (Figure 2). The single crystals of **4a**

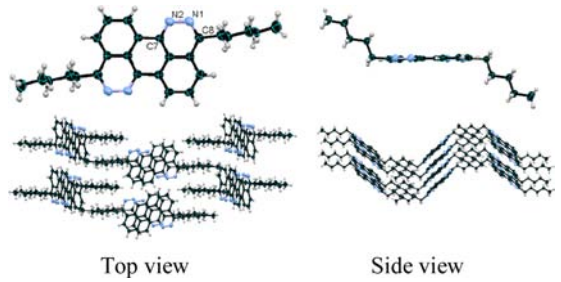

Figure 2. Crystal structures and packing diagrams for **4a**.

suitable for X-ray single-crystal analysis were obtained by slowly diffusing hexane into dichloromethane solution at room temperature. The backbone of **4a** shows a small dihedral angle of 1.2° between the central benzene ring and the outer aromatic ring. Each of the terminal butyl groups is oriented away from the rigid backbone, with a dihedral angle of around 99°. The bond length of 1.37 Å between two nitrogen atoms, and bond lengths of about 1.32 Å for C−N bonds, are obviously shorter than the corresponding C−C bond length of perylene (~1.39 Å),[11] which can be attributed to the electronegativity of nitrogen atom and the higher polarity of the C−N bonds. In addition, the C−C bond lengths in **4a** are very close to those in perylene. The packing diagram of **4a** reveals a herringbone packing motif, consisting of slipped π-stacked columns, which are strongly interdigitated with each other through side alkyl chains. As expected, the exposed N atoms of the diazine unit in **4a** facilitate the formation of intermolecular hydrogen bonds between the two parallel adjacent columns, with the bond lengths of H···N: 2.69 and 2.76 Å. Moreover, within each π-stacked column, the shortest distance of 3.40 Å between the neighboring molecules manifests a significant $\pi-\pi$ stacking interaction. Therefore, a close-packed structure in the solid state can be concluded for **4a**. Obviously, incorporation of nitrogen atoms into PAHs dramatically changes the molecular polarity, enriches the intermolecular interactions, and thus plays an important role in the crystal engineering of organic semiconductors.

UV−vis absorption spectra of **4a**,**b**, **11a**,**b**, and perylene were measured in $CHCl_3$ (Figure 3a). For **4a** and **4b** with alkyl

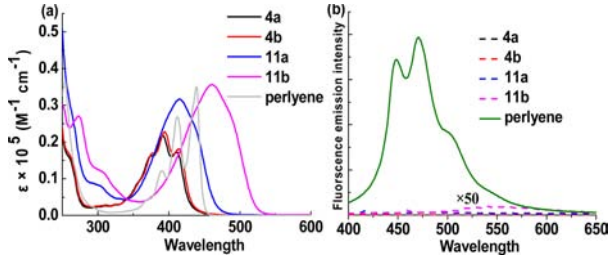

Figure 3. UV−vis absorption spectra (a) and emission spectra (b) of **4a**,**b**, **11a**,**b**, and perylene (5×10^{-5} M) in $CHCl_3$.

substitutions, a set of well-resolved absorption bands appear around 372, 390, and 410 nm, and a small shoulder peak at around 350 nm is observed. The ultraviolet regions typically originate from the $\pi-\pi^*$ transitions of the aromatic skeletons in a conjugated system, which show remarkable blue shifts in comparison to perylene with four main peaks located at 370,

dx.doi.org/10.1021/ol502109y | *Org. Lett.* 2014, 16, 4726−4729

390, 411, and 439 nm. Remarkably, apart from the high energy bands (<350 nm) in the near-ultraviolet regions which can be assigned to the $\pi-\pi^*$ transitions of the aromatic structures, **11a** and **11b** exhibit the broad featureless absorption bands with maximum peaks at 416 and 460 nm, respectively. Compared to **11a**, the maximum absorption peak of **11b** is red-shifted by 44 nm, manifesting its pronounced π-conjugated system. This red shift can be ascribed to the substitution of electron-rich thiophene groups and the increased planarity of the molecules by comparison with that of phenyl substitution in **11a**. Notably, the absorption spectra of all compounds exhibit an almost solvent-independent effect, revealing their nonpolar characters in the ground state (Figures S1−4, Supporting Information). Compound **4b** with branched alkyl side chains exhibits much better film-forming capability than the other three compounds. Red shifts and peak broadening of the absorption spectra can be observed for **4a**,**b** and **11a**,**b** in thin films compared with their absorption in solution, revealing increased electronic interaction between molecules in solid state (Figure S5, Supporting Information).[12] The UV−vis absorption spectra of these compounds were further calculated at TD-DFT level (Figures S12−16, Supporting Information), which are in good agreement with the experimental results, indicating that the main absorption bands in the low-energy spectral domain are dominated by electronic transitions between HOMO and LUMO orbitals. In addition, all four tetraazaperylene molecules show very weak fluorescence emissions in $CHCl_3$, in stark contrast to perylene with high luminescence efficiency (Figure 3b). The poor emissions of these molecules, similar to other nitrogen-embedded acenes, are probably caused by a strong trapping effect[13] or intersystem crossing effect from electron-withdrawing nitrogen-containing moieties.[14] These four molecules have nearly the same fluorescence lifetime ($\tau \sim 1.6$ ns), which is much smaller than the $\tau = 4.9$ ns for perylene (Table S1 and Figure S7−11, Supporting Information).[15]

Further insight into the electrochemical behavior of these compounds was provided by cyclic voltammetry (CV) measurements (Figure 4). In the CV profiles of **4a**,**b** and **11a**, a reversible one-electron reduction was observed, whereas the redox peaks in the second reduction process were not well-resolved. Compound **11b** exhibited two consecutive reversible one-electron reductions, demonstrating that 1,2,7,8-tetraazaperylene-cored skeleton has a fully conjugated system, and thus, the electron can be effectively delocalized over the whole molecular backbone. We

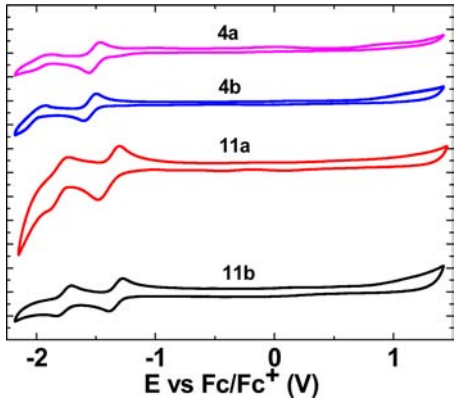

Figure 4. Cyclic voltammogram of **4a**,**b** and **11a**,**b** measured in CH_2Cl_2 (0.1 mol/L n-Bu_4NPF_6) at a scan rate of 100 mV/s. Potentials are given against ferrocene/ferrocenium ion couple (Fc/Fc^+).

did not observe any oxidation potential within the electrochemical window under the experimental conditions for all four target compounds. The reason can be attributed to the tetraazaperylene core with strong electron-deficient character, which leads to a deep-lying HOMO energy level. The reduction potentials of the first waves are gradually increase in a sequence of **4b** (−1.53 V) < **4a** (−1.50 V) < **11a** (−1.42 V) < **11b** (−1.32 V). Accordingly, the lowest unoccupied molecular orbitals (LUMO) energy values in an order of **4b** (−3.27 eV) > **4a** (−3.30 eV) > **11a** (−3.38 eV) > **11b** (−3.48 eV) are among those of typical air-stable n-type organic semiconductors.[16] Moreover, the highest occupied molecular orbitals (HOMO) energy levels are evaluated on the basis of the LUMO values and the optical band gaps, resulting in a sequence of **4a** (−6.19 eV) < **4b** (−6.14 eV) < **11a** (−5.99 eV) < **11b** (−5.83 eV) (Table 1). Therefore, the electronic structures of these molecules can be finely tuned by varying the substitution on the tetraazaperylene core.

Table 1. Electrochemical Properties of Compounds 4a,b and 11a,b

	LUMO[a] (eV)	HOMO[b] (eV)	E_g^{opt}[b] (eV)	LUMO[c] (eV)	HOMO[c] (eV)	Eg[c] (eV)
4a	-3.30	-6.19	2.89	-2.86	-6.16	3.30
4b	-3.27	-6.14	2.87	-2.82	-6.12	3.30
11a	-3.38	-5.99	2.61	-2.88	-5.94	3.05
11b	-3.48	-5.83	2.35	-3.04	-5.79	2.75

[a]LUMO = $-E_{red1}$ − 4.80 eV, E_{red1}: the first reduction potential, evaluated from half potential; [b]HOMO = LUMO − E_g^{opt}, E_g^{opt}: optical band gap, estimated from UV−vis absorption edge; [c]Obtained by DFT calculations..

To shed light on the geometric and electronic structures of such compounds, theoretical calculations based on density functional theory (DFT) (RB3LYP/6-31G (d) level) have been performed. All of the compounds show nearly flat backbones (Figure 5 and Figure S18, Supporting Information). As expected,

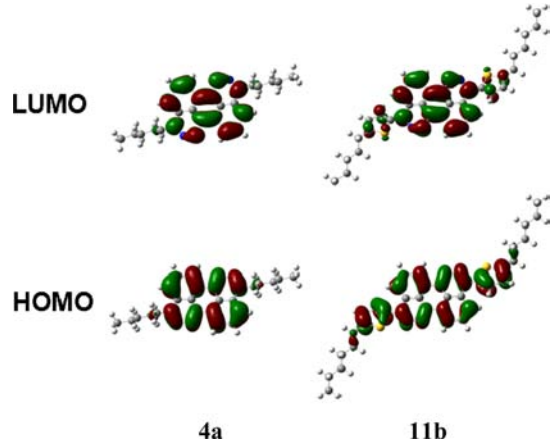

Figure 5. Calculated molecular orbital of **4a** and **11b**.

the LUMOs for all compounds primarily reside on the tetraazaperylene core, partly contributed by the benzene and thiophene rings in **11a** and **11b**, respectively, suggesting the intrinsic electron-deficient nature of the tetraaza-perylene. The HOMOs for all four compounds are fully distributed over the whole conjugated backbone, revealing that the π-electrons are

dx.doi.org/10.1021/ol502109y | Org. Lett. 2014, 16, 4726−4729

effectively delocalized on the molecular skeleton. The calculated LUMO and HOMO values are summarized in Table 1, which are accordance with the experimental results discussed above.

In conclusion, we demonstrated an efficient synthesis of a new family of electron-deficient 1,2,7,8-tetraazaperylene derivatives. Our experimental and theoretical investigations revealed that the introduction of the heteroatoms in the perylene backbone exerts remarkable influence on the optical properties and electrochemical behavior. The electron-deficient tetraazaperylene core may serve as an appealing building block for preparing conjugated oligomers and polymers with a donor−acceptor structure. The applications of these extended conjugated systems can be foreseen in various electronic devices, such as OFETs and OSCs. On the other hand, the intrinsic Lewis basicity of the diazine moiety in 1,2,7,8-tetraazaperylene derivatives may allow them to sense organic acids by selective capture of protons within a certain pK_a range. The exploration of these applications is currently ongoing in our laboratory.

■ ASSOCIATED CONTENT

Supporting Information

Experimental details, NMR spectra, UV−vis spectra, fluorescence spectra, cyclic voltammetry, and single-crystal X-ray diffraction data. This material is available free of charge via the Internet at http://pubs.acs.org

■ AUTHOR INFORMATION

Corresponding Authors

*fan-zhang@sjtu.edu.cn.
*feng@mpip-mainz.mpg.de.

Notes

The authors declare no competing financial interest.

■ ACKNOWLEDGMENTS

We acknowledge funding support from the Natural Science Foundation of China (NSFC 21174083, 2012CB933400, 2013CBA01600), the Shanghai Committee of Science and Technology (11JC1405400), the Shanghai Pujiang Program (12PJ1405300), FNRS, and EU GENIUS project. We thank Professor Xiaoli Zhao from East China Normal University for crystal X-ray diffraction and Instrumental Analysis.

■ REFERENCES

(1) (a) Anthony, J. E. *Angew. Chem., Int. Ed.* **2008**, *47*, 452. (b) Figueira-Duarte, T. M.; Müllen, K. *Chem. Rev.* **2011**, *111*, 7260. (c) Sun, Z.; Ye, Q.; Chi, C.-Y.; Wu, J.-S. *Chem. Soc. Rev.* **2012**, *41*, 7857. (d) Zhang, Z.-R; Lei, T.; Yan, Q.-F; Pei, J.; Zhao, D.-H. *Chem. Commun.* **2013**, *49*, 2882. (e) Kim, J.-H.; Song, C. E.; Kang, I.-N.; Shin, W. S.; Hwang, D.-H. *Chem. Commun.* **2013**, *49*, 3248. (d) Mateo-Alonso, A. *Chem. Soc. Rev.* **2014**, *43*, 6311.

(2) Jiang, W.; Li, Y.; Wang, Z.-H. *Chem. Soc. Rev.* **2013**, *42*, 6113.

(3) (a) Bunz, U. H. F.; Engelhart, J. U.; Lindner, B. D.; Schaffroth, M. *Angew. Chem., Int. Ed.* **2013**, *52*, 3810. (b) Appleton, A. L.; Brombosz, S. M.; Barlow, S.; Sears, J. S.; Bredas, J.-L.; Marder, S. R.; Bunz, U. H. F. *Nat. Commun.* **2010**, *1*, 91. (c) Liu, Y.-Y.; Song, C.-L.; Zeng, W.-J.; Zhou, K.-G.; Shi, Z.-F.; Ma, C.-B.; Yang, F.; Zhang, H.-L.; Gong, X. *J. Am. Chem. Soc.* **2010**, *132*, 16349. (d) Liang, Z.-X; Tang, Q.; Xu, J.-B; Miao, Q. *Adv. Mater.* **2011**, *23*, 1535.

(4) Rieger, R.; Müllen, K. *J. Phys. Org. Chem.* **2010**, *23*, 315.

(5) Tokita, S.; Hiruta, K.; Kitahar, K.; Nishi, H. *Synthesis* **1982**, 229.

(6) Jiang, W.; Zhou, Y.; Geng, H.; Jiang, S.-D; Yan, S.-K; Hu, W.-P; Wang, Z.-H; Shuai, Z.-G; Pei, J. *J. Am. Chem. Soc.* **2010**, *133*, 1.

(7) Fan, J.; Zhang, L.; Briseno, A. L.; Wudl, F. *Org. Lett.* **2012**, *14*, 1024.

(8) Duerr, B. F.; Chung, Y. S.; Czarnik, A. W. *J. Org. Chem.* **1988**, *53*, 2120.

(9) Wei, X.; Tong, W.; Fidler, V.; Zimmt, M. B. *J. Colloid Interface Sci.* **2012**, *387*, 221.

(10) (a) Ogawa, S.; Muraoka, H.; Kikuta, K.; Saito, F.; Sato, R. *J. Organomet. Chem.* **2007**, *692*, 60. (b) Zheng, X.-J; Lu, S.-L; Li, Z.-P. *Org. Lett.* **2013**, *15*, 5432.

(11) Li, R.-J; Hu, W.-P; Liu, Y.-Q; Zhu, D.-B. *Acc. Chem. Res.* **2010**, *43*, 529.

(12) Jiang, J.-Y; Kaafarani, B. R.; Neckers, D. C. *J. Org. Chem.* **2006**, *71*, 2155.

(13) Liu, Y.-Q; Zhang, F.; He, C.-F.; Wu, D.-Q.; Zhuang, X.-D; Xue, M.-Z; Liu, Y.-G; Feng, X.-L. *Chem. Commun.* **2012**, *48*, 4166.

(14) Schmidt, K.; Brovelli, S.; Coropceanu, V.; Beljonne, D.; Cornil, J.; Bazzini, C.; Caronna, T.; Tubino, R.; Meinardi, F.; Shuai, Z.; Brédas, J.-L. *J. Phys. Chem. A* **2007**, *111*, 10490.

(15) (a) Ruetten, S. A.; Thomas, J. K. *J. Phys. Chem. B* **1998**, *102*, 598. (b) Katoh, R.; Sinha, S.; Murata, S.; Tachiya, M. *J. Photochem. Photobiol. A* **2001**, *145*, 23.

(16) (a) Liang, Z.-X; Tang, Q.; Mao, R.-X; Liu, D.-Q; Xu, J.-B; Miao, Q. *Adv. Mater.* **2011**, *23*, 5514. (b) Gawrys, P.; Marszalek, T.; Bartnik, E.; Kucinska, M.; Ulanski, J.; Zagorska, M. *Org. Lett.* **2011**, *13*, 6090.